

2017 Electrical Insulation Conference (EIC), Baltimore, MD, USA, 11 - 14 June 2017

Corrosion Current Level Estimation of Rust Samples using Inverse Dielectric Spectroscopy

Jones Owusu Twumasi¹ and Tzuyang Yu²

¹Doctoral Candidate

²Associate Professor, Ph.D.

Email: Tzuyang_Yu@uml.edu

^{1,2}Department of Civil and Environmental Engineering, UMass Lowell, Lowell, MA 01854, USA

Abstract— Dielectric spectroscopy is a standard technique used for characterizing the energy storage and dissipation properties of dielectrics and has been applied for a wide range of fields in science and engineering. In civil engineering, dielectric properties of construction materials can be used for quality assurance (e.g., mechanical strength) and structural health monitoring (e.g., corrosion detection). In the corrosion detection problem of reinforced concrete structures, level of corrosion current is crucial to the accurate estimation of corrosion level (amount of rust) and is typically challenging to measure without destructively damaging the integrity of concrete. In this paper, a new technique based on inverse dielectric spectroscopy is proposed to estimate the current level in artificial corrosion. To achieve the goal, artificially accelerated corrosion products (rust samples) were developed. In artificially accelerated corrosion experiment, three externally supplied corrosion current levels (0.25 A, 0.50 A, and 0.75 A) were applied to steel specimens inside a corrosion reactor, and the rust samples were collected for dielectric spectroscopy measurement (dielectric constant and loss factor) in the microwave frequency range of 0.5 ~ 4.5 GHz using a dielectric coaxial probe (Agilent 85070E) and a network analyzer (Agilent E5071C). An inverse dielectric spectroscopy model incorporating loss factor, measurement frequency and corrosion current level was developed from the artificially corroded rust samples. From our experimental result, it is found that i) the higher the corrosion current level, the lower the dielectric constant and loss factor of artificial rust in the measured frequency range; and ii) corrosion current level inside artificial rust can be estimated by using an inverse dielectric spectroscopy model.

Keywords—dielectric properties, corrosion, rust, microwave, corrosion current level

I INTRODUCTION

Corrosion current level is one of the most important parameters for predicting corrosion rate or understanding corrosion mechanism of steel reinforcing bar (rebar) inside reinforced concrete (RC) structures. Accurate measurement/prediction of corrosion rate is useful in evaluating the extent and the progress of corrosion damage in RC structures [1]. Present methods for corrosion rate measurement include polarization resistance, open circuit potential, electrochemical impedance, or concrete resistance measurements [2]. Most of these methods are qualitative, partially-quantitative, and rely on the electrochemical reaction within RC structures for corrosion rate prediction [2].

Recently, characterization of rust samples as a means of quantifying corrosion rate and corrosion damage inside RC structures has gained attention. Garcia et al. [3] found that corrosion rates are higher when rust samples contain large quantities of certain iron oxide compounds (e.g. akaganeite,

lepidocrocite, and goethite). Furthermore, characterization of rust samples by Marcotte [4] revealed that, volume of iron oxide compounds ranges from 2-6 times of the volume of original steel. In addition, Shinohara [5,6] has reported that increase in overall steel volume due to rust samples induces tensile forces at the steel-concrete interface, as one of the primary causes of concrete cracking in RC structures. Also, Zhao *et al.* [7] applied x-ray diffraction and thermal analysis on rust samples and found that differences in the composition of rust samples are responsible for variation in different corrosion environments. Morales *et al.* [8] also found that large quantities of magnetite in rust samples are associated with higher corrosion rates.

Although the dielectric properties (dielectric constant and loss factor) of rust samples (e.g., magnetite-Fe₃O₄, goethite – FeO(OH), hematite – Fe₂O₃, maghemite γ -Fe₂O₃) have been studied [9-15], the relationship between dielectric properties of rust samples and corrosion current level is unclear in literature. Such relationship will be useful in predicting and quantifying corrosion rate of steel rebar inside concrete. Kim et al. [9] measured the dielectric properties of four factory-manufactured rust samples in the frequency range of 0.5 ~ 6 GHz and two other rust samples harvested from a corroded steel bridge girder and steel rebars inside concrete beam in the frequency range of 0.5 ~ 12 GHz, to aid the detection and quantification of steel rebar corrosion using electromagnetic (EM) /radar sensors.

In this study, dielectric properties of rust samples obtained from artificial corrosion were measured using a dielectric coaxial probe (Agilent 85070E) and a network analyzer (HP/Agilent E5071C) in the frequency range of 0.5 ~ 4.5 GHz. We investigated the effect of corrosion current level on the dielectric properties of rust samples obtained artificially, and modeled the corrosion current level as a function of loss factor of rust samples and measurement frequency.

II. EXPERIMENTAL PROGRAM

A. Specimen description

Three No.4 steel rebar specimens (nominal diameter =12.7 mm) with a length of 200 mm were artificially corroded at three different impressed current levels inside sodium chloride (NaCl) solution and their rust samples were collected. Table 1 describes all specimens used in this research.

B. Accelerated corrosion test and rust collection procedure

Impressed current accelerated corrosion test (ACT) was used in this study to corrode steel rebar specimens within a

short period of time. The steel rebar specimens were submerged inside 5% (by mass) NaCl solution. A direct current power supply (Tekpower HY1803D, 0~18 V, 0~3 A) was used to impress a constant current on the steel rebar specimens. A non-conductive container was used to store the NaCl solution (electrolyte). In each ACT, the steel rebar specimen was used as the anode, while a copper tube was used as the cathode. Average temperature and relative humidity were 26°C and 45%, respectively. At the end of each ACT, the rust samples inside the corrosion reactor were filtered out and allowed to air dry. The dry rust samples in the form of flakes were grounded into powder before measuring their dielectric properties.

Table 1. Specimen description

Sample	Corrosion current level (A)	Corrosion scheme
C250	0.25	Artificial
C500	0.50	Artificial
C750	0.75	Artificial

C. Dielectric measurements

Dielectric constant and loss factor of three rust samples were measured using an open-ended coaxial probe (Agilent 85070E) and a network analyzer (HP/Agilent E5071C) [16,17] in the frequency range of 0.5 ~ 4.5 GHz. The details of calibration of the dielectric measurement system can be found in the literature [16]. Measured dielectric constants and loss factors are shown in Fig. 1.

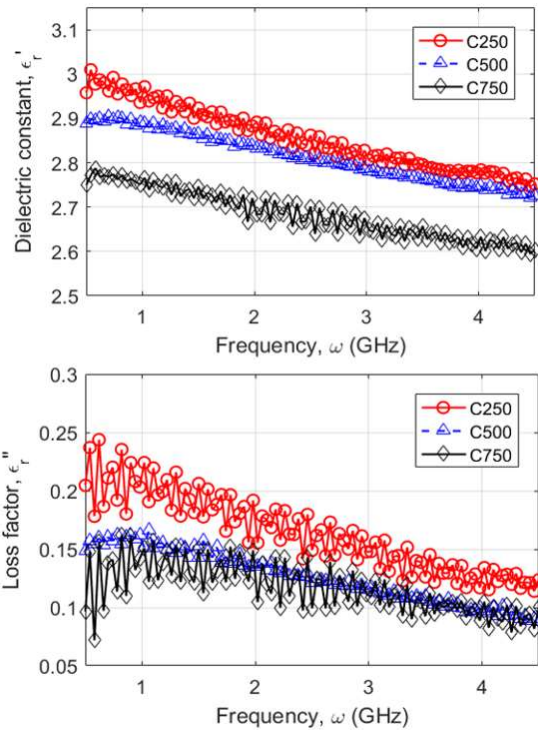


Fig. 1 Dielectric constant and loss factor measurements of artificial rust samples C250, C500, and C750

III. RESULT

From our experiments, it was observed that the dielectric constant and loss factor of our rust samples in the frequency

range of 0.5 ~ 4.5 GHz decrease nonlinearly when measurement frequency increases (Fig. 1). Dielectric constant curves of rust samples (C250 and C750) demonstrated much less fluctuations than their loss factor curves, except for rust sample C500 whose dielectric constant and loss factor curves were both stable. On the other hand, the increase of corrosion current level resulted in the decrease of both dielectric constant and loss factor measurements for all rust samples in the frequency range of 0.5 ~ 4.5 GHz, although proportionality was not held in the relations between corrosion current and dielectric properties (dielectric constant and loss factor) in our experiments.

IV. INVERSE DIELECTRIC MODELING

In the inverse dielectric modeling of this paper, corrosion current level (I) of artificial rust samples between 0.25 ~ 0.75 A was predicted from their dielectric properties in the frequency range of 0.5 ~ 4.5 GHz. This is achieved by adopting the approach in [17]. In this approach, Debye's model (Eqs. (1) and (2)) was rearranged such that corrosion current (I) becomes a function of loss factor and measurement frequency.

$$\epsilon'_r(\omega) = \epsilon_\infty + \frac{\epsilon_0 - \epsilon_\infty}{1 + (\omega\tau)^2} \quad (1)$$

$$\epsilon''_r(\omega) = \frac{\omega\tau(\epsilon_0 - \epsilon_\infty)}{1 + (\omega\tau)^2} \quad (2)$$

$$I(\omega, \epsilon''_r) = \frac{B + \sqrt{B^2 - 4AC}}{2A} \quad (3)$$

where

$$A(\omega, \epsilon''_r) = c_6^2 \omega^2 \epsilon''_r + (c_4 c_6 - c_2 c_6) \omega \quad (4)$$

$$B(\omega, \epsilon''_r) = 2c_5 c_6 \omega^2 \epsilon''_r + (c_4 c_5 - c_2 c_5 - c_1 c_6 + c_3 c_6) \omega \quad (5)$$

$$C(\omega, \epsilon''_r) = \epsilon''_r + c_5^2 \omega^2 \epsilon''_r - (c_1 c_5 - c_3 c_5) \omega \quad (6)$$

and ω = measurement frequency (GHz), $\epsilon_0(I) = c_1 - c_2 I$ (static dielectric constant at $\omega = 0$), $\epsilon_\infty(I) = c_3 - c_4 I$ (infinite dielectric constant at $\omega = \infty$), $\tau(I) = c_5 - c_6 I$ (relaxation time (ns)), I = corrosion current level ($0.25 \leq I \leq 0.75$ A), $c_1, c_2, c_3, c_4, c_5,$ and c_6 = model coefficients (Table 2). In this approach, corrosion current dependency was first modeled with Debye's model parameters ($\epsilon_\infty, \epsilon_0, \tau$). Loss factor (Eq. (2)) was then represented by corrosion current (I) and inversed to obtain the corrosion current expression. Eq. (3) predicts the corrosion current level of rust samples, using measurement frequency (0.5~4.5 GHz) and loss factor. The reason for choosing loss factor is because loss factor (imaginary part of the complex electric permittivity) is directly associated with the electric conductivity of rust samples. In other words, loss factor is more sensitive to the variation in impressed corrosion current levels than dielectric constant.

Table 2. Coefficients of the proposed corrosion current model.

Coefficient	c_1	c_2	c_3	c_4	c_5	c_6
Value	3.19	0.549	2.693	0.259	1.018	0.35

V. FINDINGS

A. Dielectric constant of rust

It was found that dielectric constant measurements of

artificial rust samples decrease with increase in measurement frequency in the range of 0.5~4.5 GHz, indicating that the rust samples are dielectrically dispersive (Fig. 1). The use of Debye's model appeared to be a viable approach for modeling the dielectric constant of artificial rust samples. Figs. 2~4 show the performance of proposed dielectric constant model (Eq. (1)).

B. Loss factor of rust

Loss factor measurements of artificial rust samples also demonstrated dielectric dispersion in the frequency range of 0.5~4.5 GHz. It was measured that the loss factor of rust decreased with the increase of measurement frequency. While the loss factor of rust shares similar dielectric dispersion phenomenon with the dielectric constant of rust, it experimentally showed more fluctuation in two rust samples (C250 and C750). The level of loss factor fluctuation also appeared to decrease with the increase of frequency. In other words, more fluctuation is associated with the loss factor of rust at lower frequencies (0.5~1.5 GHz) and less fluctuation with higher frequencies (3.5~4.5 GHz). Modeling the loss factor of artificial rust using Debye's model provided satisfactory performance in the frequency range of 1.5~4.5 GHz (Figs. 2~4). Higher errors were associated with predicted loss factor in the frequency range of 0.5~1.5 GHz when using Debye's model.

C. Corrosion current level

From our experiments, we found that corrosion current level has a negative impact on the magnitude of both dielectric constant and loss factor of artificial rust samples. The increase of corrosion current level resulted in the decrease of both dielectric constant and loss factor of artificial rust samples. In other words, the lower the corrosion current level, the higher the dielectric constant and loss factor values. This indicates that C250 contains greater proportions of magnetite (which has high dielectric constant [8]) than C500 and C750. The dielectric constant of rust sample C750 with the highest corrosion current (C750 = 0.75 A) was the lowest among other dielectric constant measurements of rust samples C250 and C500.

D. Corrosion current level modeling

From the inverse dielectric model for predicting corrosion current level of artificial rust samples, it was found that Debye's model parameters (ϵ_0 , ϵ_∞ , τ) can be linearly related to the corrosion current level of artificial rust. Static dielectric constant ϵ_0 , infinite dielectric constant ϵ_∞ , and relaxation time τ all linearly decrease with the increase of corrosion current I . Fig. 5 illustrates the predicted relations between measurement frequency vs. corrosion current and loss factor vs. corrosion current. Our inverse dielectric model suggests that same loss factor value of artificial rust can be achieved by different combinations of corrosion current levels and measurement frequencies.

VI. CONCLUSION

We measured and analyzed the dielectric properties of artificial rust samples in the frequency range of 0.5 ~ 4.5 GHz and proposed an inverse model for predicting corrosion

current level in artificial rust. Loss factor of artificial rust was used in the model development, in view of its theoretical relationship with electric conductivity. From our experimental data, both dielectric constant and loss factor of artificial rust nonlinearly decrease with corrosion current level. In addition, different combinations of corrosion current levels and measurement frequencies can predict the same loss factor value of artificial rust.

ACKNOWLEDGMENT

This work was performed partially under the support of the National Science Foundation, the Civil, Mechanical and Manufacturing Innovation (CMMI) Division, through a grant CMMI-1401369 (PI: Prof. Xingwei Wang, UMass Lowell). The authors want to thank undergraduate student Christopher Ingemi for his help with experimental work.

REFERENCE

- [1] Otieno, M. B., Beushausen, H. D., & Alexander, M. G. (2011). Modelling corrosion propagation in reinforced concrete structures—a critical review. *Cement and Concrete Composites*, 33(2), 240-245.
- [2] Song, H. W., & Saraswathy, V. (2007). Corrosion monitoring of reinforced concrete structures—a. *Int. J. Electrochem. Sci*, 2, 1-28.
- [3] Garcia, K. E., Morales, A. L., Arroyave, C. E., Barrero, C. A., & Cook, D. C. (2003). Mössbauer characterization of rust obtained in an accelerated corrosion test. *Hyperfine interactions*, 148(1-4), 177-183.
- [4] Marcotte, T. D. (2001). Characterization of Chloride-Induced Corrosion Products that form in Steel-Reinforced Cementitious. PhD Thesis in Mechanical Engineering. University of Waterloo: Waterloo, Canada
- [5] Shinohara, Y. (2010). Crack initiation and propagation caused by corrosion-product expansion around corroding bars. In K. van Breugel, G. Ye, & Y. Yuan (Eds.), *2nd International Symposium on Service Life Design for Infrastructures* (pp. 623-630). RILEM Publications SARL.
- [6] Shinohara, Y. (2011). Effect of Confinement upon Crack Behaviors caused by Corrosion-Product Expansion around Corroding Bars. In *Proceedings of the 12nd International Conference on Durability of Building Materials and Components* (Vol. 3, pp. 1577-1584).
- [7] Zhao, Y., Ren, H., Dai, H., & Jin, W. (2011). Composition and expansion coefficient of rust based on X-ray diffraction and thermal analysis. *Corrosion Science*, 53(5), 1646-1658.
- [8] Morales, A. L., Cartagena, D., Rendon, J. L., & Valencia, A. (2000). The relation between corrosion rate and corrosion products from low carbon steel. *physica status solidi (b)*, 220(1), 351-356.
- [9] Kim, S., Surek, J., & Baker-Jarvis, J. (2011). Electromagnetic metrology on concrete and corrosion. *Journal of research of the National Institute of Standards and Technology*, 116(3), 655.
- [10] Iwauchi, K., Yamamoto, S., Bando, Y., Hanai, T., Koizumi, N., Takada, T., & Fukushima, S. (1971). Dielectric Properties of the Mixtures of α -Fe₂O₃, TiO₂ and Fe₂TiO₅. *Japanese Journal of Applied Physics*, 10(11), 1513.
- [11] Onari, S., Arai, T., & Kudo, K. (1977). Infrared lattice vibrations and dielectric dispersion in α -Fe₂O₃. *Physical Review B*, 16(4), 1717.
- [12] Chen, Y. J., Gao, P., Wang, R. X., Zhu, C. L., Wang, L. J., Cao, M. S., & Jin, H. B. (2009). Porous Fe₃O₄/SnO₂ core/shell nanorods: synthesis and electromagnetic properties. *The Journal of Physical Chemistry C*, 113(23), 10061-10064.
- [13] Nikolic, M. V., Slankamenac, M. P., Nikolic, N., Sekulic, D. L., Aleksic, O. S., Mitric, M., ... & Nikolic, P. M. (2012). Study of dielectric behavior and electrical properties of hematite α -Fe₂O₃ doped with Zn. *Science of Sintering*, 44(3), 307-321.
- [14] Lunt, R. A., Jackson, A. J., & Walsh, A. (2013). Dielectric response of Fe₂O₃ crystals and thin films. *Chemical Physics Letters*, 586, 67-69.
- [15] Ghayour, H., Abdellahi, M., Bahmanpour, M., & Khandan, A. (2016). Simulation of dielectric behavior in RFeO₃ orthoferrite ceramics (R= rare earth metals). *Journal of Computational Electronics*, 15(4), 1275-1283.
- [16] Yu, T. Y. (2011). Dielectric deamplification of multiphase cementitious composites in the frequency range of 0.5 GHz to 4.5 GHz. In *2011 Electrical Insulation Conference (EIC)*. (pp. 313-317). IEEE.
- [17] Twumasi, J. O., & Yu, T. (2015). Forward and inverse dielectric modeling of oven-dried cement paste specimens in the frequency range

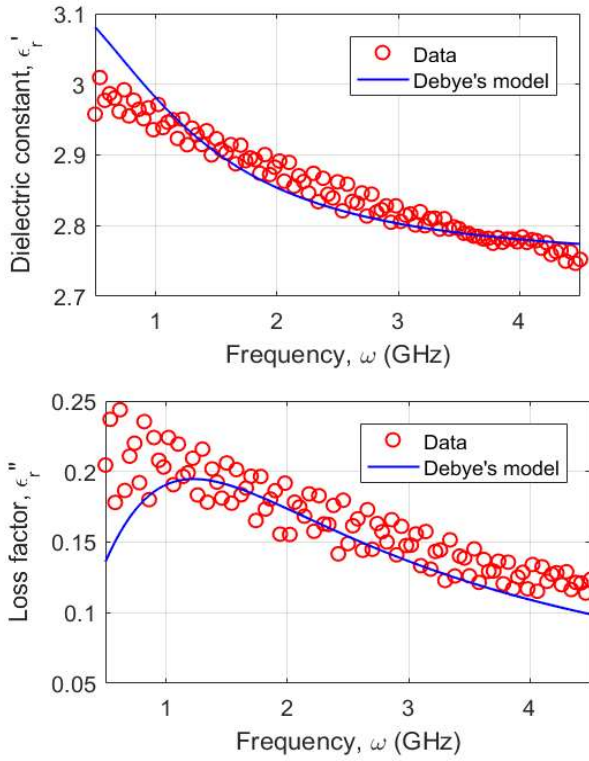


Fig. 2. Comparison between Debye's model and measured dielectric constant and loss factor measurement of artificial rust sample C250

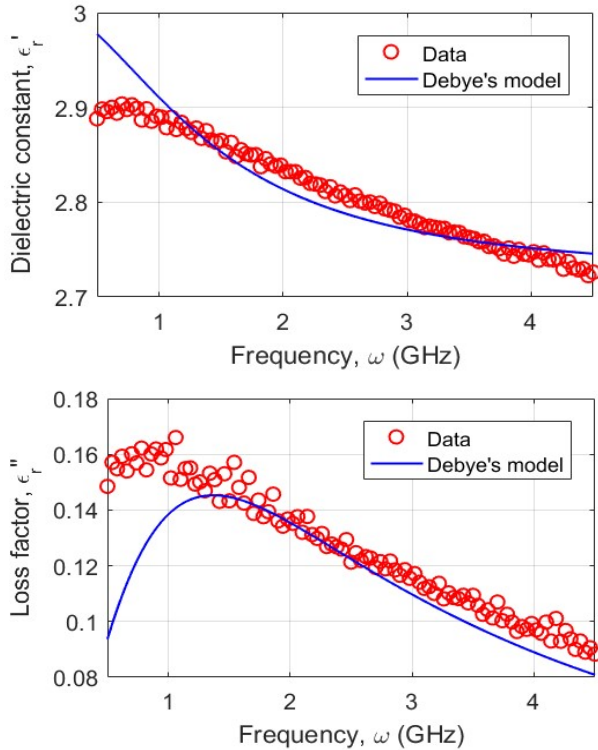


Fig. 3. Comparison between Debye's model and measured dielectric constant and loss factor measurement of artificial rust sample C500

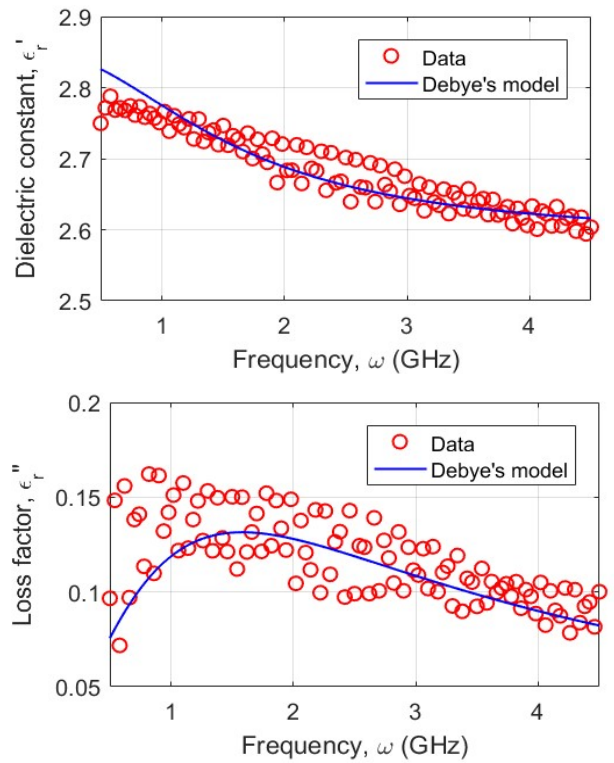


Fig. 4. Comparison between Debye's model and measured dielectric constant and loss factor measurement of artificial rust sample C750

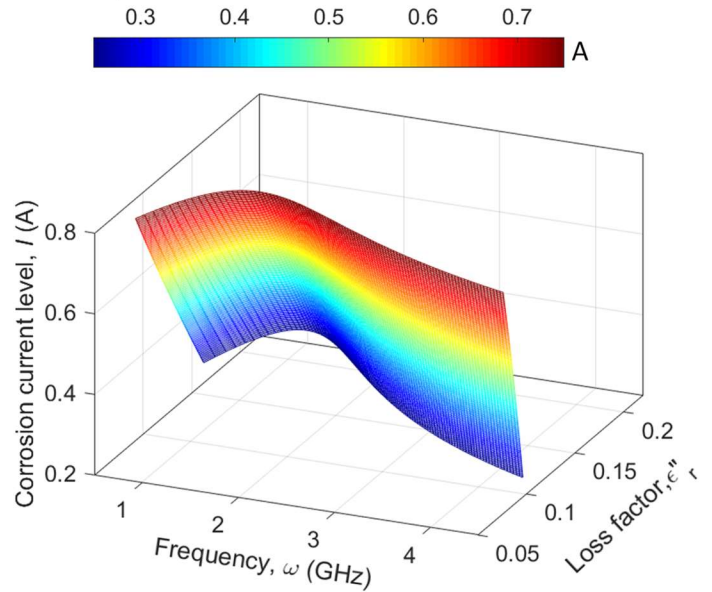


Fig. 5. Relationship between corrosion current level, measurement frequency and loss factor